Food Research International 228 (2026) 118268

Contents lists available at ScienceDirect

Food Research International

journal homepage: www.elsevier.com/locate/foodres

Elucidation of molecular interactions between selected phenylpropanoids and myofibrillar protein: Conformational remodeling and machine learning analysis

Jingfan Wang [a,b], Laiyu Zhao [a], Ping Yang [a], Tianze Wang [a], Ying Xu [a], Dong Han [a,*], Marie-Laure Fauconnier [b], Giorgia Purcaro [c], Chunhui Zhang [a,*]

[a] Key Laboratory of Agro-Products Processing, Ministry of Agriculture and Rural Affairs, Institute of Food Science and Technology, Chinese Academy of Agricultural Sciences, Beijing 100193, China
[b] Laboratory of Chemistry of Natural Molecules, Gembloux Agro-Bio Tech, University of Liege, 5030 Gembloux, Belgium
[c] Laboratory of Analytical Chemistry, Gembloux Agro-Bio Tech, University of Liège, 5030 Gembloux, Belgium

ARTICLE INFO

Keywords:
Beef protein
Structural character
Spice flavors

ABSTRACT

Phenylpropanoid flavor compounds (PFCs) are major contributors to the characteristic herbal and anise-like aromas of stewed beef with spices (SBS). This study investigated the binding interactions between five PFCs and myofibrillar proteins (MPs) under varying heat and concentration conditions. Heat treatment partially unfolded MPs, thereby exposing thiol groups and hydrophobic regions that enhanced PFC binding. In unheated MPs, the addition of PFCs increased α-helix content by promoting hydrogen bond formation driven by hydrophobic interactions; however, prolonged heating attenuated these effects due to protein aggregation that restricted access to binding sites. The distinct binding behaviors among the five PFCs were successfully characterized using machine learning–based clustering models. K-means clustering analysis revealed distinct binding behaviors of eugenol (EG) and anethole (AT) toward MPs, compared with methyleugenol (ME), estragole (ET), and anisaldehyde (AL). The two clusters were consistent with the binding energy of molecular docking. Disruption agent tests and molecular docking revealed hydrophobic interactions as the main driving force for PFCs-MP binding. Structural differences among PFCs, such as hydroxyl group positions, affected their hydrogen bonding and steric accessibility. Overall, thermally induced protein conformational changes play a crucial role in flavor retention, thereby informing flavor management during meat product processing.

1. Introduction

Aroma plays a vital role in the perception and enhancement of food quality. The retention and controlled release of aroma in thermally processed meat are critical challenges in food stability, especially in traditional products such as stewed beef with spices (SBS) (Bortnowska, 2024). The intensity of aroma in the headspace is influenced by the physicochemical properties of both the aroma and the meat matrix, their interaction qualities, and environmental conditions, such as temperature and concentration (Bortnowska, 2024). Myofibrillar proteins (MPs), the major structural proteins in muscle tissues, could interact with aroma to promote the overall flavor characteristics of meat products (Sun et al., 2024). The physicochemical properties of MPs play a vital role in improving meat products' texture and flavor (Zhao et al., 2022). As natural carriers of flavor compounds, MPs provide a variety of chemical sites with varying interaction strengths with flavor compounds (Zhang et al., 2021). Amino acid residues primarily interact with aroma via hydrophobic, hydrogen bonding, and electrostatic forces, contributing to the stabilization of MPs–aroma complexes (Sun et al., 2024). Moreover, the conformation of MPs could be affected by the chemical characteristics of ligand aroma compounds, which would also influence the binding behavior (Guo et al., 2020; Xiang et al., 2025). For instance, it has been reported that the binding between MPs and ketones is primarily driven by hydrophobic forces (Wang et al., 2022). The molecular

Abbreviations: PFCs, phenylpropanoids flavor compounds; SBS, stewed beef with spices; MPs, myofibrillar protein; ME, methyleugenol; EG, eugenol; ET, estragole; AT, anethole; AL, anisaldehyde; UH, unheated treatment; HU, heat up treatment; CD, cool down treatment..

* Corresponding authors.
E-mail addresses: orange_1101@126.com (D. Han), dr_zch@163.com (C. Zhang).

https://doi.org/10.1016/j.foodres.2025.118268
Received 6 November 2025; Received in revised form 25 December 2025; Accepted 26 December 2025
Available online 5 January 2026

polarity and the position of branched chains within the furan structures contribute to different binding behavior between MPs and furan derivatives (Yin et al., 2022).

Phenylpropanoids flavor compounds (PFCs) are derived from spices, which are widely used in SBS processing due to their distinctive sensory properties. Our previous research focused on the identification of key aroma-active compounds in SBS (Wang, Wang, et al., 2024; Wang, Yang, et al., 2024). Phenylpropanoid flavor compounds (PFCs)—such as eugenol, estragole, anethole, anisaldehyde, and methyleugenol—are dominant contributors to the herbal and anise-like aroma of SBS (Wang, Wang, et al., 2024; Wang, Yang, et al., 2024). Spices commonly used during SBS processing, such as clove, cinnamon, fennel, and star anise, are well-documented sources of the major phenylpropanoids examined in this study. For example, cloves (*Syzygium aromaticum*) have exceptionally high levels of eugenol and methyl eugenol, which confer them their characteristic warm, spicy aroma (Cortés-Rojas et al., 2014). Similarly, estragole, anethole, and anisaldehyde are prevalent in herbs and spices like fennel (*Foeniculum vulgare*) and star anise (*Illicium verum*) (Dief et al., 2025). The structural feature of PFCs is a benzene ring substituted with a three-carbon side chain, enabling their participation in diverse molecular interactions (Schieber & Wust, 2020). These substituents may include phenolic hydroxyl groups (e.g., eugenol), methoxy groups (e.g., estragole, anethole, and methyl eugenol), and aldehyde moieties (e.g., anisaldehyde). This structural variation gives rise to a mechanistically relevant spectrum of hydrogen-bonding ability, electrophilicity, and hydrophobicity. It was reported that conformational alterations in MPs induced by etheric compounds contribute to a less compact three-dimensional gel network, thereby promoting the release of aldehydes (Sun et al., 2024). As previously reported, the binding affinity of PFCs to proteins is influenced by factors including molecular weight, hydroxylation, and methylation of PFCs (Ozdal et al., 2013). Moreover, functional groups such as hydroxyl and methoxy make PFCs particularly reactive toward proteins (Chen et al., 2020). Key aroma-active PFCs exhibit substantial structural and conformational diversity. At every stage of SBS processing, PFCs inevitably interact with MPs within the meat matrix, potentially leading to alterations in flavor quality. Therefore, elucidating the interaction mechanisms between MPs and PFCs is essential for controlling and improving the flavor characteristics of SBS. Additionally, the impact of conformational differences on the binding mechanisms between PFCs and MPs remains to be elucidated.

Numerous studies investigated the interactions between flavor compounds and protein (Gianelli et al., 2003; Zhou et al., 2014). As reported, model systems can elucidate flavor binding mechanism to explore factors, such as the physicochemical properties of aroma compounds, concentration, and temperature that influence the binding behavior (Bortnowska, 2024). It is well-documented that an increase in the chain length of aroma compounds within the same chemical class is associated with enhanced flavor retention (Lou et al., 2017). The study by Yun et al. (Yun et al., 2019) investigated the binding behavior between pyrazines and bovine serum albumin, finding that tyrosine and tryptophan residues were identified as the major binding sites for alkyl-substituted pyrazines, with binding predominantly mediated by electrostatic and hydrophobic interactions. Additionally, the structure and conformation of proteins play a crucial role in modulating their flavor-binding capacity (Zhou et al., 2014). In SBS processing, beef was first boiled for 40 min in the tanks (heat-up treatment) and then simmered by soaking in the warm marinade liquid for 150 min (cool-down treatment) (Wang, Wang, et al., 2024; Wang, Yang, et al., 2024). During heat processing, the volatility and thermal sensitivity of PFCs result in labile release and retention behavior, which would influence the sensory quality of SBS. However, a comprehensive understanding of how structural diversity among PFCs and heat-induced conformational changes in MPs influence their interactions is still unclear. Specifically, the influence of specific structural transitions of MPs on the binding behavior of key PFCs, as well as the ultimate shaping of flavor retention during industrial cooling by these interactions, is unclear. Therefore, the objectives of this research are to determine the conformational changes that MPs undergo during actual thermal–cooling processing, to elucidate the mechanism by which representative PFCs engage with MPs at the molecular level, and to clarify the role of PFCs-MPs interactions on the retention/release quality of volatile compounds. The findings will be valuable for controlling flavor in thermally processed protein-based systems, such as SBS.

2. Materials and methods

2.1. Materials

Fresh beef (*longissimus thoracis et lumborum,* slaughter ages 22–24 months, slaughter weights 350–400 kg, the carcasses were aged at 4 °C) was purchased from a local supermarket. PFCs (ME, EG, ET, AT, AL) were obtained from Sigma-Aldrich Chemical Co. (Shanghai, China). Other chemicals were of analytical grade and were purchased from Sinopharm Chemical Reagent Co., Ltd. (Shanghai, China). The physicochemical properties of PFCs are presented in Table S1.

2.2. Extraction of myofibrillar proteins (MPs)

The MPs were extracted from beef muscle using a previously reported method (Bortnowska, 2024) with modifications. In brief, the minced muscle was homogenized in phosphate extraction solution (PES, 0.1 M NaCl, 1 mM EGTA, 2 mM $MgCl_2$, 10 mM $Na_3PO_4{\cdot}12H_2O$, pH 7) for 15 s at 12,000 rpm (three times, with intermittent intervals of 15 s) and then centrifuged at 3000 ×*g*, 4 °C for 15 min. After two additional washes under the same conditions, the myofibril pellet underwent three further washes with a 0.1 M NaCl solution. The MPs were stored at 4 °C for a maximum of 48 h. Before further analysis, the MPs were diluted to the target concentration using pre-chilled phosphate buffer solution (PBS, 20 mM Na_2HPO_4, 0.6 M NaCl, pH 7). A Bicinchoninic acid (BCA) protein assay kit (Solarbio, Beijing, China) was used to determine the protein concentration.

2.3. Preparation of heated MPs

MPs were adjusted to 4 mg/mL with PBS. The protein solution was divided into 33 aliquots. The prepared MP solutions were allocated to a total of 33 treatment conditions: 3 heat levels (UH, unheated; HU, heat up, boilied to 85 °C and keep 10 min; CD, cool down, boiled to 85 °C keep 10 min and then simmered at 45 °C for 30 min) × 5 phenylpropanoids flavor compounds (ME; EG; ET; AT; AL) × 2 concentrations (0.05 mM; 1 mM) +3 control (UH, HU, CD). As shown in Fig.S1, the heating parameters were set in terms of the heating rate of industrial processing. After treatments, the samples were promptly cooled with ice water and then stored in the 4 °C refrigerator before further analysis. The specific processing conditions corresponding to the various groups are detailed in Table S2.

2.4. The impact of PFCs on the MPs' structure

2.4.1. Protein surface hydrophobicity, total sulfhydryl, and free amine groups determination

The surface hydrophobicity was determined as described by Yang et al. (2024), with a slight modification. Different groups (containing 1 mL of 2 mg/mL MPs) and the control group (containing 1 mL of PBS) were vortexed for about 30 s after the addition of 200 μL bromophenol blue (BPB, 1 mg/mL). The mixture was shaken for 15 min at 25 ± 1 °C, followed by centrifugation at 4000 ×*g* for 15 min at 25 °C. After centrifugation, 1 mL of the supernatant was diluted with 9 mL of PBS. This diluted sample was subsequently subjected to absorbance measurement at 595 nm. Surface hydrophobicity was assessed by quantifying the BPB bound, calculated according to the following equation:

$$\textbf{Bound BPB}\ (\mu g) = 200 \times \frac{OD_{ck} - OD_{MPs}}{OD_{ck}}$$

OD_{ck} and OD_{MPs} showed different absorbance values at 595 nm between the blank group and the experimental group.

According to (Yang et al., 2024), the DTNB reaction was employed to measure the total sulfhydryl content of MPs. The protein solution was analyzed at an absorption wavelength of 412 nm, with an extinction coefficient of 13,600 M^{-1} cm^{-1}. The content of free amine ($-NH_2$) groups (FAG, nmol/mg protein) was determined following the TNBS method described by Bortnowska (2024). Absorbance at 420 nm was measured, and the FAG contents were calculated from a calibration curve prepared with L-leucine.

2.4.2. Circular dichroism spectroscopy

A MOS-450/AF-CD spectrometer (Bio-Logic, France) was used to record the circular dichroism spectroscopy of the MPs (0.5 mg/mL) as previously described (Chai et al., 2025). The spectra were recorded over a wavelength range of 190–260 nm. The secondary structures of the MPs were calculated using DichroWeb (Miles et al., 2022).

2.4.3. Fluorescence spectroscopy

The experiments were carried out based on the methodology described by Bortnowska (2022), with minor modifications. MP solution (0.2 mg/mL) was prepared by diluting with 20 mM PBS. Aroma compounds were individually added to vials containing the MPs solution. A control sample containing only the MPs was also prepared. Fluorescence emission spectra were obtained over the range of 300–450 nm using an excitation wavelength of 280 nm (Bortnowska, 2022).

2.4.4. Particle size

The particle size (*Z*-average) was analyzed by Zetasizer Nano-ZS (Malvern Instruments, Malvern, Worcestershire, UK). The MP solution (1 mg/mL) was analyzed at 25 °C with a scattering angle of 90°. The dispersion medium consisted of 50 mM phosphate buffer (pH 7.0) containing 0.6 M NaCl, with its refractive index adjusted to 1.33. The relative refractive index and absorption index were set to 1.414 and 0.001, respectively.

2.4.5. Sodium dodecyl sulfate-polyacrylamide gel electrophoresis (SDS-PAGE)

Protein solution (2 mg/mL) was mixed in a 1:1 (*v*/v) ratio with Laemmli sample buffer (Bio-Rad, Hercules, CA, USA). The mixture was denatured (5 min, 100 °C) and clarified by centrifugation (15,000 ×*g*, 15 min, 4 °C). Aliquots (10 μL) of supernatants and 5 μL of protein standards were loaded on a precast polyacrylamide gel (12.5 % separating, 5 % stacking; Biotides Biotechnology, Beijing, China) using SDS-PAGE. Proteins were visualized using Coomassie blue R-250 staining (2 h) followed by overnight destaining. The gel was photographed using ChemiDocTM MP software.

2.5. Binding behavior of PFCs to MPs

2.5.1. Determination of binding percentages

The protein–aroma binding ability was conducted on the method of Wang, Wang, et al. (2024); Wang, Yang, et al. (2024). Stock solutions of the PFCs were obtained by dissolving each compound in methanol to a final concentration of 10 mM. These solutions were then added to the MPs solution (4 mg/mL) and the control solution (20 mM PBS), resulting in a gradient concentration for each aroma compound (0, 0.01, 0.02, 0.04, 0.08, 0.16, 0.2, 0.4, 0.6, 0.8, and 1 mM). An aliquot (5 mL) from the mixture was placed into 20 mL headspace vials, sealed with PTFE-lined silicone septa, and kept at 4 °C for 12 h to reach equilibrium.

For the extraction of volatile compounds, a divinylbenzene/carboxen/polydimethylsiloxane (DVB/CAR/PDMS) fiber (50/30 m, 2 cm, Supelco, Bellefonte, PA, USA) was used at 25 °C for 30 min. The analysis of volatiles was conducted by GC − MS (Agilent 8860, Santa Clara, CA, U.S.A) equipped with a DB-Wax capillary column (30 m × 0.18 mm × 0.18 μm; Agilent, Santa Clara, CA, U.S.A). The fiber was thermally desorbed in splitless mode at 250 °C for 3 min. The GC oven program began with an initial hold at 35 °C for 3 min, followed by a ramp of 5 °C /min to 210 °C. Mass spectrometric detection was performed in electron impact (EI) mode at 70 eV, scanning *m/z* 35–400, with the ion source temperature set at 230 °C.

The binding percentages was determined by calculating as the ratio of free volatile compounds in the headspace, using the following formula (Wang & Arntfield, 2015):

$$\text{Free volatile compounds}\ (\%) = \frac{peak\ area^{with\ protein\ added}}{peak\ area^{without\ protein\ added}} \times 100\%$$

2.5.2. K-means clustering algorithms for binding behavior classification

Following the theoretical framework of clustering algorithms proposed in previous research (Ezugwu et al., 2022), K-means was applied to categorize the binding ability of PFCs. The clustering models were constructed and visualized using Metabo Analyst 6.0.

2.5.3. Chemical bonds

We employed guanidine hydrochloride (GuHCl, disrupting hydrophobic interactions, hydrogen bonding, and ionic effects), propylene glycol (PG, suppressing hydrophobic forces but enhancing hydrogen bonding), urea (disrupting hydrogen bonding and hydrophobic interactions), $Cl_3CCOONa$ (destabilizing protein structure) and DTT (reducing inter- and intramolecular S—S bonds) to probe interaction mechanisms (Wang & Arntfield, 2016). The chemical interactions of MPs were analyzed based on the methods of Bortnowska (2024) with slight modifications. Contents of PFCs were determined as described in Section 2.5.1.

2.6. Atomic force microscopy (AFM)

MPs were diluted to a concentration of 0.25 mg/mL. A 10 μL sample from each group was deposited onto freshly peeled mica and left to air-dry on a clean bench, forming an MP adsorption layer.

2.7. Molecular docking

The crystal structure of myosin (PDB: 8QYU) was obtained from the Protein Data Bank. The three-dimensional structures of PFCs were retrieved from PubChem (ME, PubChem ID: 7127; EG, PubChem ID: 3314; ET, PubChem ID: 8815; AT, PubChem ID:637563; AL, PubChem ID:31244). Molecular docking investigations were conducted on AutoDock Vina. A total of ten docking poses were generated for each ligand. The optimal conformation for each ligand-receptor pair was identified using the Vina scoring function, and subsequent inspection was conducted to ascertain interaction patterns. Ligand-receptor interaction analyses were performed using Ligplus and PyMOL, including hydrogen bonding, hydrophobic interactions, and key residue contacts.

2.8. Statistical analysis

All experiments were performed in triplicate. Data were displayed as mean ± standard errors (SE). General linear model program and One-way analysis of variance (ANOVA) in IBM SPSS 26.0 (SPSS Inc., Chicago, USA) was conducted for analysis. Before conducting parametric tests, we confirmed the normality of the data distribution using the Shapiro–Wilk test and checked for homogeneity of variance using Levene's test. If the assumptions were violated, the Welch's ANOVA was applied. A significance level of $P < 0.05$ was considered statistically significant.

3. Results and discussion

3.1. Changes of amino acid residue side-chain groups

3.1.1. Total sulfhydryl content

Sulfhydryl groups, abundant on side chains of MPs' amino acids, are highly reactive and susceptible to oxidation. Determination of total sulfhydryl content was a critical index for evaluating changes in the antioxidant capacity of MPs and redox state of thiol groups (Jia et al., 2017). As shown in Fig. 1-(A), the reduction of total sulfhydryl content was observed after the addition of PFCs in the UH treatment ($P < 0.05$). Furthermore, sulfhydryl groups might deprotonate to produce mercaptide ions (RS-), which then react with carbonyl groups (Han et al., 2021). Moreover, it was reported that the decrease indicated that PFCs preferentially interacted with cysteine residues in the myosin heavy chain (Han et al., 2022; Strauss & Gibson, 2004). Total sulfhydryl content was significantly increased in the CD group (Fig. 1-(C)). Heating can induce conformational stretching of MPs, leading to the exposure of formerly buried sulfhydryl groups (Cao et al., 2019). The hydrophobicity of PFCs may synergistically intensify conformational changes in the low-temperature stewing, thereby increasing the detectable sulfhydryl content. Compared with other PFCs, MPs treated with EG had the lowest sulfhydryl content, indicating that the molecular structure of PFCs can affect their binding behavior with MPs. EG contains a phenolic hydroxyl group, which can form quinone derivatives. This EG quinone derivative readily reacts with the nucleophilic sulfhydryl groups of MPs, leading to covalent adduct formation (Chen, Ma, et al., 2023; Chen, Zhao, et al., 2023).

3.1.2. Free amine content

To assess the degree of protein oxidation and associated structural changes, ε-NH_2 groups of lysine side chains were assessed by free amine content (Chen, Ma, et al., 2023; Chen, Zhao, et al., 2023). The PFCs-induced free amine changes of the UH treatment were shown in Fig. 1-(D). The low-concentration group significantly increased the free amine content, whereas the high-concentration group significantly reduced the free amine content. In the low concentration groups, PFCs may promote partial structural unfolding of MPs by interacting with hydrophobic regions, thereby increasing the exposure of ε-amino groups on lysine residues. In contrast, PFCs-induced protein aggregation or triggered covalent binding enhanced the loss of free amine groups in high concentrations. This decreasing trend is consistent with the results reported by Prodpran et al. (2012), who demonstrated that tannic acid led to a significant reduction in the free amine content of fish MPs. The observed concentration-dependent impact of PFCs on free amine content was not evident in the two heated groups. This discrepancy is likely attributable to the influence of heat treatment on the structural properties of MPs. Heat may promote protein aggregation and cross-linking, effectively masking reactive amine sites. Consequently, the interaction between PFCs and protein-bound amines becomes limited, diminishing

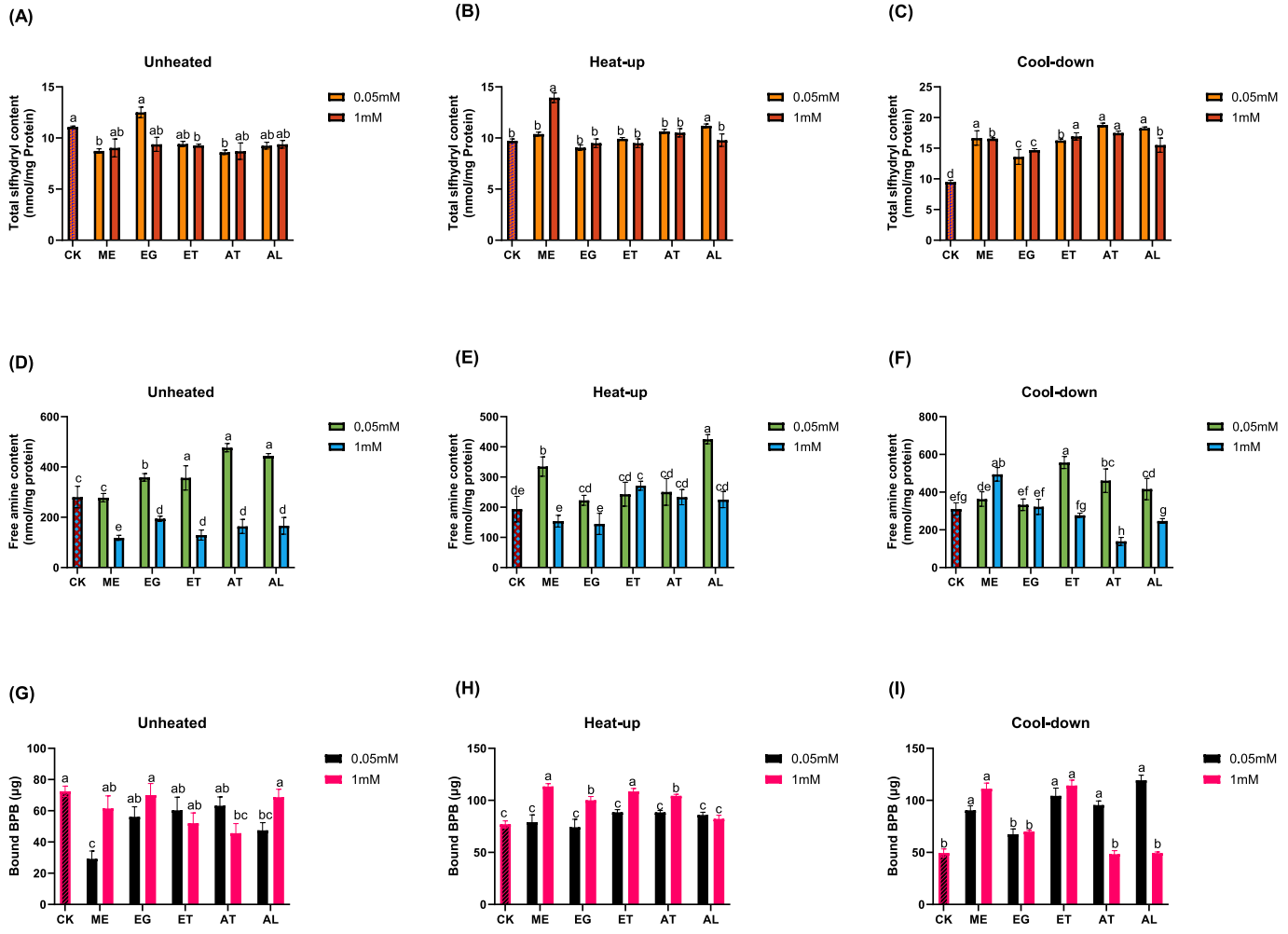

Fig. 1. Total sulfhydryl content (A, Unheated; B, Heat-up; C, Cool-down), free amine content (D, Unheated; E, Heat-up; F, Cool-down), BPB-bound content (G, Unheated; H, Heat-up; I, Cool-down). CK, control group; ME, methyleugenol; EG, eugenol; ET, estragole; AT, anethole; AL, anisaldehyde. Columns with different letters indicate a significant difference ($P < 0.05$).

the concentration-dependent effect observed in other treatments. In contrast, the stewing process involves gradual heating, which may reduce the extent of irreversible aggregation. This could allow for maintaining the observed concentration-response trend in the UH group. Non-covalent interactions between the aromatic rings or hydroxyl groups of PFCs and amino acid side chains may reduce the detectability of free amine groups (Xu, Dong, et al., 2020; Xu, Wang, et al., 2020). AL, containing an aldehyde group, may also react with amine groups through nucleophilic addition. Notably, EG, as a phenolic compound with hydroxyl groups, is prone to oxidation, generating quinones that react with free amines to form C—N bonds (Chen, Ma, et al., 2023). The covalent amine-quinone adduction may also result in the reduction of amine groups. Additionally, oxidation of the ε-NH_2 groups of lysine residues resulted in the formation of carbonyl derivatives. These reactive carbonyls can further interact with available amino groups, thereby leading to an additional decrease of free amine content (Levine et al., 1990). Previous study also reported that the addition of rutin at varying concentrations could influence interactions between MPs–MPs and MPs–rutin, leading to the reduction of free amine groups and promoting gelation ability of MPs (Jia et al., 2019).

3.2. Changes in the secondary structure of MPs

Circular dichroism is commonly used to determine protein conformational changes quickly and sensitively. Circular dichroism was employed in the far-ultraviolet range to investigate the secondary structure alterations of MPs combined with PFCs (190–260 nm). As shown in Table 1, heat treatment significantly altered myofibrillar protein secondary structures, with α-helix content increasing and β-sheet reduction ($P < 0.05$). The results of our study align with a previous study conducted by Chen, Ma, et al., 2023; Chen, Zhao, et al., 2023. Heat-induced unfolding disrupted intermolecular hydrogen bonds stabilizing β-sheets, while liberated polypeptide segments refold into α-helices stabilized by intramolecular H-bonds (Ju et al., 2023). According to previous studies, temperature-dependent oxidation generates carbonyl groups and aromatic residues (Trp/Tyr/Phe), which may promote an increase in the α-helix contents (Dockal et al., 2000). The results showed that the addition of PFCs to unheated MPs caused an enhancement in α-helix content. Which is likely due to the insertion of PFCs into hydrophobic pockets, leading to the formation of stabilizing non-covalent interactions such as hydrophobic contacts and hydrogen bonds (Sun et al., 2023). These interactions have been shown to restrict protein backbone flexibility, thereby favoring the maintenance of native helical conformations and promoting intramolecular hydrogen bonding (Xu et al., 2021). However, following thermal treatment, heat-induced unfolding disrupts the native tertiary and secondary structures of MPs, exposing hydrophobic cores and causing irreversible aggregation, thereby diminishing the ability of PFCs to stabilize α-helices (Xiang et al., 2025). In summary, the impact of heat on protein architecture suggests that the responsiveness to small-molecule stabilization by phenylpropanoids is diminished. This phenomenon elucidates the observation that PFCs exert a weaker influence on α-helix content in heated systems.

3.3. Changes in the tertiary structure of MPs

3.3.1. Surface hydrophobicity

Surface hydrophobicity was employed to analyze the surface alterations of the protein molecule. As presented in Fig. 1, PFCs showed distinct binding behaviors under varying concentrations and thermal conditions. In the UH treatment, the low-concentration groups of ME and AL exhibited a significant surface hydrophobicity reduction ($P < 0.05$). In the HU treatment, the surface hydrophobicity of the high-concentration groups was notably enhanced. Heat treatment increased MPs' secondary structure unfolding degree, leading to the exposure of hydrophobic groups (Cao et al., 2019). The synergistic effect of the

Table 1
Protein secondary structure content of MPs under different treatments.

PFC	Concentration	Heat	Total α-helix	Total β-sheets	Total β-turn	Total random coil
CK	0 mM	Unheated	10.15 ± 0.19^{d}	45.65 ± 0.13^{a}	10.58 ± 0.08^{c}	33.62 ± 0.04^{a}
		Heat-up	42.22 ± 1.3^{a}	14.79 ± 0.46^{b}	17.35 ± 0.49^{a}	25.63 ± 0.34^{b}
		Cool-down	38.55 ± 1.45^{a}	16.83 ± 1.09^{a}	18.21 ± 0.01^{a}	26.44 ± 0.38^{a}
ME	0.05 mM	Unheated	34.99 ± 0.12^{a}	19.14 ± 0.16^{c}	18.64 ± 0.05^{b}	27.30 ± 0.04^{d}
		Heat-up	37.17 ± 0.80^{c}	17.42 ± 0.69^{a}	18.55 ± 0.18^{a}	26.96 ± 0.17^{a}
		Cool-down	38.87 ± 1.29^{a}	16.64 ± 0.70^{a}	18.12 ± 0.26^{a}	26.44 ± 0.44^{a}
	1 mM	Unheated	10.80 ± 0.26^{d}	45.44 ± 0.15^{a}	10.14 ± 0.06^{c}	33.65 ± 0.06^{a}
		Heat-up	41.01 ± 0.22^{b}	16.06 ± 0.08^{b}	17.11 ± 0.15^{b}	25.88 ± 0.03^{b}
		Cool-down	41.47 ± 1.33^{a}	15.45 ± 0.77^{b}	17.29 ± 0.27^{b}	25.76 ± 0.28^{a}
EG	0.05 mM	Unheated	33.08 ± 1.06^{a}	20.05 ± 0.40^{c}	18.82 ± 0.23^{a}	28.09 ± 0.46^{c}
		Heat-up	44.42 ± 0.39^{a}	13.96 ± 0.17^{c}	16.61 ± 0.10^{b}	25.04 ± 0.11^{b}
		Cool-down	39.14 ± 0.45^{a}	16.05 ± 0.18^{b}	18.39 ± 0.09^{a}	26.45 ± 0.17^{a}
	1 mM	Unheated	28.91 ± 3.14^{b}	23.04 ± 2.97^{a}	17.41 ± 1.96^{b}	30.67 ± 2.11^{a}
		Heat-up	39.11 ± 1.05^{b}	16.26 ± 0.45^{a}	18.22 ± 0.29^{a}	26.38 ± 0.29^{a}
		Cool-down	38.32 ± 1.05^{a}	17.06 ± 0.66^{a}	18.07 ± 0.10^{a}	26.59 ± 0.31^{a}
ET	0.05 mM	Unheated	28.51 ± 0.04^{c}	22.07 ± 0.05^{b}	20.84 ± 0.01^{a}	28.55 ± 0.01^{b}
		Heat-up	42.38 ± 1.18^{a}	14.85 ± 0.49^{b}	17.26 ± 0.38^{a}	25.51 ± 0.31^{b}
		Cool-down	38.82 ± 1.32^{a}	16.45 ± 0.67^{a}	18.19 ± 0.30^{a}	26.48 ± 0.32^{a}
	1 mM	Unheated	35.48 ± 0.15^{a}	18.54 ± 0.15^{c}	18.64 ± 0.01^{b}	27.31 ± 0.05^{d}
		Heat-up	35.40 ± 0.12^{c}	18.34 ± 0.06^{a}	18.91 ± 0.03^{a}	27.35 ± 0.10^{a}
		Cool-down	38.14 ± 0.53^{a}	16.57 ± 0.49^{a}	18.08 ± 0.14^{a}	27.11 ± 0.15^{a}
AT	0.05 mM	Unheated	32.71 ± 2.00^{a}	19.98 ± 1.08^{c}	19.32 ± 0.60^{a}	27.98 ± 0.40^{c}
		Heat-up	38.99 ± 2.64^{b}	16.78 ± 1.30^{a}	17.88 ± 0.59^{a}	26.38 ± 0.66^{a}
		Cool-down	41.42 ± 2.57^{a}	15.80 ± 1.64^{b}	16.95 ± 0.33^{b}	25.79 ± 0.63^{a}

(continued on next page)

Table 1 (*continued*)

PFC	Concentration	Heat	Total α-helix	Total β-sheets	Total β-turn	Total random coil
	1 mM	Unheated	30.46 ± 0.56^{b}	21.10 ± 0.25^{b}	19.97 ± 0.44^{a}	28.48 ± 0.09^{b}
		Heat-up	37.82 ± 0.28^{c}	16.88 ± 0.27^{a}	18.53 ± 0.10^{a}	26.81 ± 0.09^{a}
		Cool-down	35.74 ± 0.36^{b}	18.42 ± 0.24^{a}	18.39 ± 0.19^{a}	27.42 ± 0.09^{a}
AL	0.05 mM	Unheated	32.20 ± 0.19^{b}	20.28 ± 0.12^{c}	19.12 ± 0.24^{a}	28.40 ± 0.02^{c}
		Heat-up	39.41 ± 0.98^{b}	16.11 ± 0.39^{a}	18.19 ± 0.27^{a}	26.33 ± 0.36^{a}
		Cool-down	39.52 ± 0.36^{a}	15.90 ± 0.18^{b}	18.30 ± 0.10^{a}	26.28 ± 0.16^{a}
	1 mM	Unheated	29.55 ± 1.17^{b}	21.52 ± 0.69^{b}	20.25 ± 0.58^{a}	28.61 ± 0.34^{b}
		Heat-up	36.75 ± 1.45^{c}	17.66 ± 0.86^{a}	18.59 ± 0.21^{a}	27.00 ± 0.39^{a}
		Cool-down	39.64 ± 1.24^{a}	16.38 ± 0.90^{a}	17.82 ± 0.04^{b}	26.19 ± 0.29^{a}

addition of PFCs was observed in the low-concentration groups in Fig. 1-(H) and (I). The aggregation of MPs induced by PFCs may reduce the content of exposed surface hydrophobic groups and result in their re-embedding behavior, thereby effectively lowering the measurable concentration of MPs (Sun et al., 2024). On the contrary, high-concentration groups showed higher surface hydrophobicity. This may be attributed to excess PFCs destabilizing the aggregates and leading to the release of the hydrophobic surface. Particularly, MPs treated with AL exhibited a significantly lower surface hydrophobicity ($P < 0.05$). This may relate to the high binding affinity of AL to MPs. Similarly, phenolic-MPs complexes showed lower hydrophobicity because high-affinity polyphenol interactions effectively mask hydrophobic groups (Xu et al., 2021). Besides, AL is structurally distinct because of the aldehyde group, whereas the others (ME, EG, ET, and AT) primarily contain allyl side chains and methoxy substitutions. This structural difference may confer AL a greater potential to form covalent interactions, such as Schiff base linkages with amino groups (e.g., lysine residues) on proteins, leading to different binding behaviors and conformational effects compared to those of the other compounds. The unique structure of AL may make it more likely to form covalent interactions, such as Schiff base bonds, with amino groups on proteins such as lysine residues (Xu et al., 2022). Thereby, AL-induced protein cross-linking and aggregation may reduce the exposure of surface hydrophobic groups, resulting in decreased BPB-binding capacity (Huang et al., 2022). The structural differences of PFCs may result in different surface hydrophobicity alterations of the protein.

3.3.2. Fluorescence spectroscopy

Tryptophan residues usually reside in the hydrophobic core of well-folded proteins and display strong intrinsic fluorescence. However, unfolding of MPs can lead to the exposure of tryptophan (Trp) residues to the aqueous environment, resulting in a reduction in fluorescence intensity (Sun et al., 2024). According to Fig. 2-(A), compared to the HU group, the fluorescence intensity of the CD group increased, suggesting that Trp residues had transitioned into a more hydrophobic environment. High-temperature treatment can cause partial unfolding of MPs, exposing buried Trp residues in the hydrophobic region (Sun et al., 2024). During the subsequent low-temperature incubation, partial refolding or aggregation may occur, allowing Trp residues to become re-embedded in less polar, hydrophobic regions. Consequently, this unfolding-refolding structural transition reduces solvent exposure and dynamic quenching by water molecules, leading to a blue shift in the emission peak (Li et al., 2022). The addition of PFCs resulted in a noticeable enhancement in the fluorescence intensity of HU-MPs, suggesting that a common structural feature—a substituted aromatic ring with hydrophobic alkyl or allyl side chains—enables them to insert into the hydrophobic regions of thermally unfolded MPs effectively. AL, which possesses an aldehyde group and lacks the hydrophobic side chain, has reduced hydrophobicity, resulting in weaker insertion into hydrophobic pockets.

3.4. Protein profiles

The thermal degradation and aggregation behavior were further assessed by SDS-PAGE analysis. MPs were predominantly composed of myosin heavy chain (MHC), actin, and myosin light chain (MLC) (Fig. 2-(B)). Protein bands were identified based on the research of Wang et al. (2023). For the UH group, the binding intensity of MHC, actin, and MLC decreased with the addition of PFCs, which may result from protein intermolecular aggregation induced by the interaction of PFCs with hydrophobic regions of MPs. Compared with the UH and HU groups, the CD group showed an increase in bands, indicating degradation of MPs into smaller polypeptides or amino acids during prolonged stewing (Wang et al., 2023). Similarly, Tajima et al. (2006) observed that heat treatment induced degradation of MHC into lower molecular weight fragments. Notably, the binding intensity of heated MPs decreased after adding EG (Fig. 2-(B)). As concentration increased, this decrease became more pronounced. The concentration-dependent reduction of dissociated MHC bands may indicate progressive MPs degradation (Ge et al., 2018). MPs partially unfolded with heating denaturation, which exposed reactive groups such as thiols and hydrophobic groups. EG may reduce protein aggregation by stabilizing these reactive groups through non-covalent interactions. This may prevent large aggregate formation, resulting in smaller protein particles, consistent with the particle size reduction of EG. In contrast, the MHC binding intensity and polymers of heated MPs increased after adding AL (Fig. 2-(B)). That is, AL may be attributed to increased solubility or reduced aggregation of MHC following treatment.

3.5. Particle size

Particle size is associated with protein aggregation. As presented in Fig. 2-(C), the addition of PFCs increased the particle size of UH-MPs, suggesting the formation of larger aggregations (Huang et al., 2022). These increases may result from interactions such as secondary hydrophobic and hydrogen bonding (Promeyrat et al., 2010). Additionally, the particle size of CD-MPs was decreased with the addition of PFCs. The contrasting effects of PFCs on MPs aggregation before and after heat treatment can be attributed to the temperature-dependent conformational changes in MPs. In the UH group, the native tertiary and quaternary structures of MPs remained intact. Hydrophobic PFCs can facilitate MPs aggregation by embedding into the hydrophobic core, which would result in increased particle size (Qian et al., 2024; Xu, Dong, et al., 2020; Xu, Wang, et al., 2020). In contrast, thermal treatment alters the structure of MPs by unfolding α-helices, exposing buried hydrophobic and reactive groups. This conformational rearrangement increases the accessibility of binding sites for PFCs, which may promote the formation of stable non-covalent complexes through hydrogen bonding or van der Waals interactions (Sun et al., 2023). These interactions can spatially prevent aggregation and lead to reduced particle size. Differences in particle size between PFCs can be ascribed to the different hydrophobic interactions between specific PFCs and MPs, which differentially affect the exposure of hydrophobic regions on the MPs' surface.

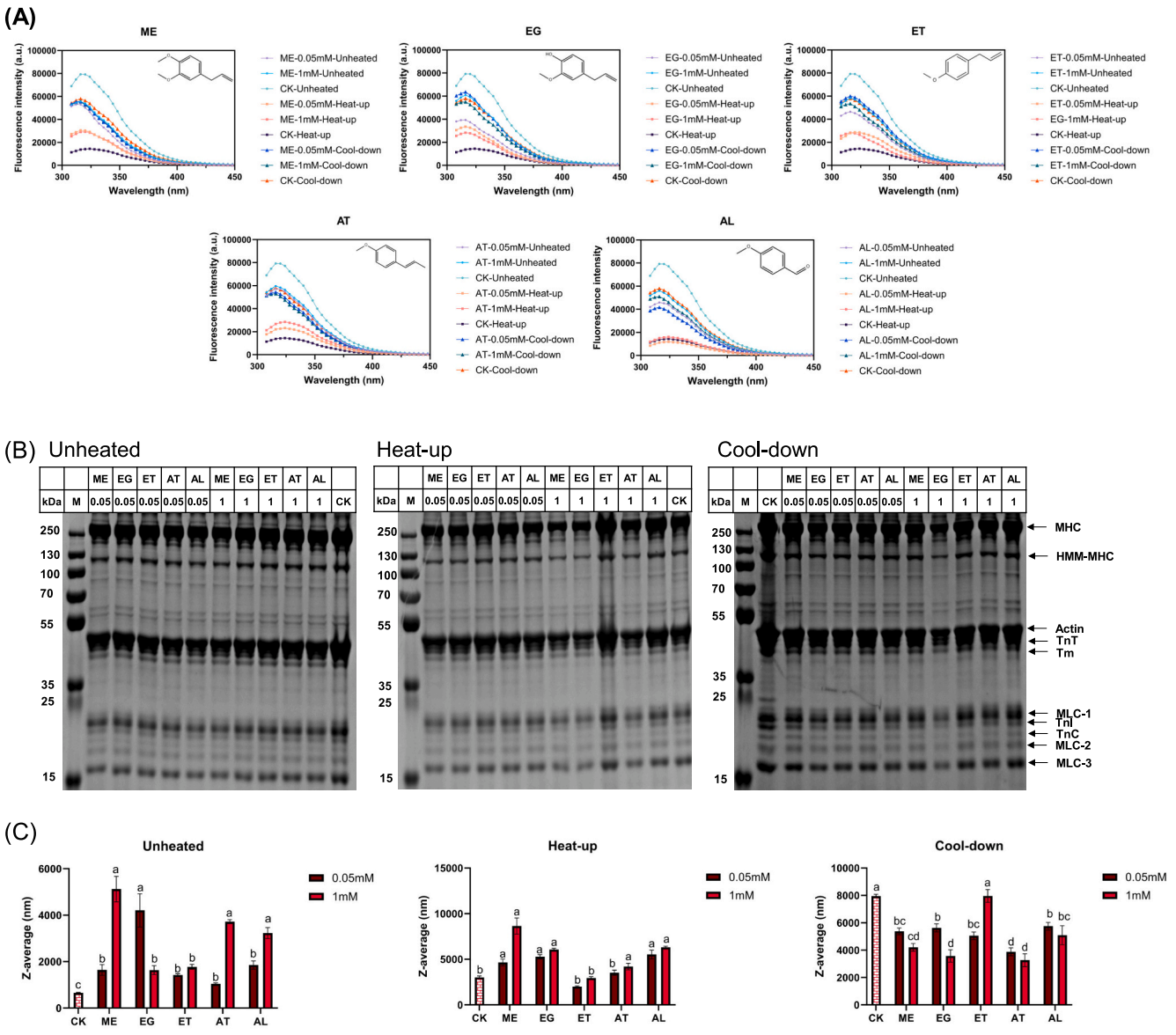

Fig. 2. (A) Fluorescence spectra of MPs with different treatments. (B) SDS-PAGE patterns of different heat treatments. Lane M, standard protein markers. MHC, myosin heavy chain; HMM-MHC, heavy meromyosin−myosin heavy chain; TnT, troponin T; Tm, tropomyosin; MLC1, myosin light chain-1; TnI, troponin I; TnC, troponin C; MLC-2, myosin light chain-2; MLC-3, myosin light chain-3. (C) Particle size of MPs with different treatments.CK, control group; ME, methyleugenol; EG, eugenol; ET, estragole; AT, anethole; AL, anisaldehyde. Columns with different letters indicate a significant difference ($P < 0.05$).

3.6. *Microstructure of MPs*

AFM was used to visualize the complex and concentration-dependent changes in the microstructure of MPs after PFCs addition (Fig. 3-(A)). Compared with CK, the addition of PFCs resulted in the aggregation of MPs. Similar structural changes were reported by Sun et al. (2024), who observed obvious aggregation in MPs' microstructure following the addition of flavor compounds. The five PFCs showed distinct influences on MPs' microstructure, due to their structural differences such as hydrophobicity, hydrogen bonding capability, and functional group reactivity. ME and ET displayed small and loosely organized protein aggregates at low concentrations, likely due to hydrophobic binding mediated by their aromatic cores and alkyl groups. With increasing concentration, ET induced stronger protein aggregation using increased clustering of the hydrophobic parts. In contrast, ME displayed larger but lower-density clusters. This phenomenon may result from the hydrophobic force promoting lateral protein-protein interactions, favoring the formation of flattened, multi-layered assemblies rather than vertically extended structures. EG and AT, which possess stronger hydrogen bonding potential through their free hydroxyl groups, exhibited a stabilizing effect on protein structures. As the concentration increased, their degree of aggregation decreased, indicating an inhibitory effect on protein aggregation by competing for interaction sites, thus stabilizing the native protein's conformation. Due to the presence of a reactive aldehyde group, AL showed a unique phenomenon. At low concentrations, AL displayed minor conformational changes, possibly resulting from its Schiff base formation with surface-exposed lysine residues of MPs (Yu et al., 2025). However, the degree of crosslinking increased at higher concentrations, which may result in the formation of large aggregates.

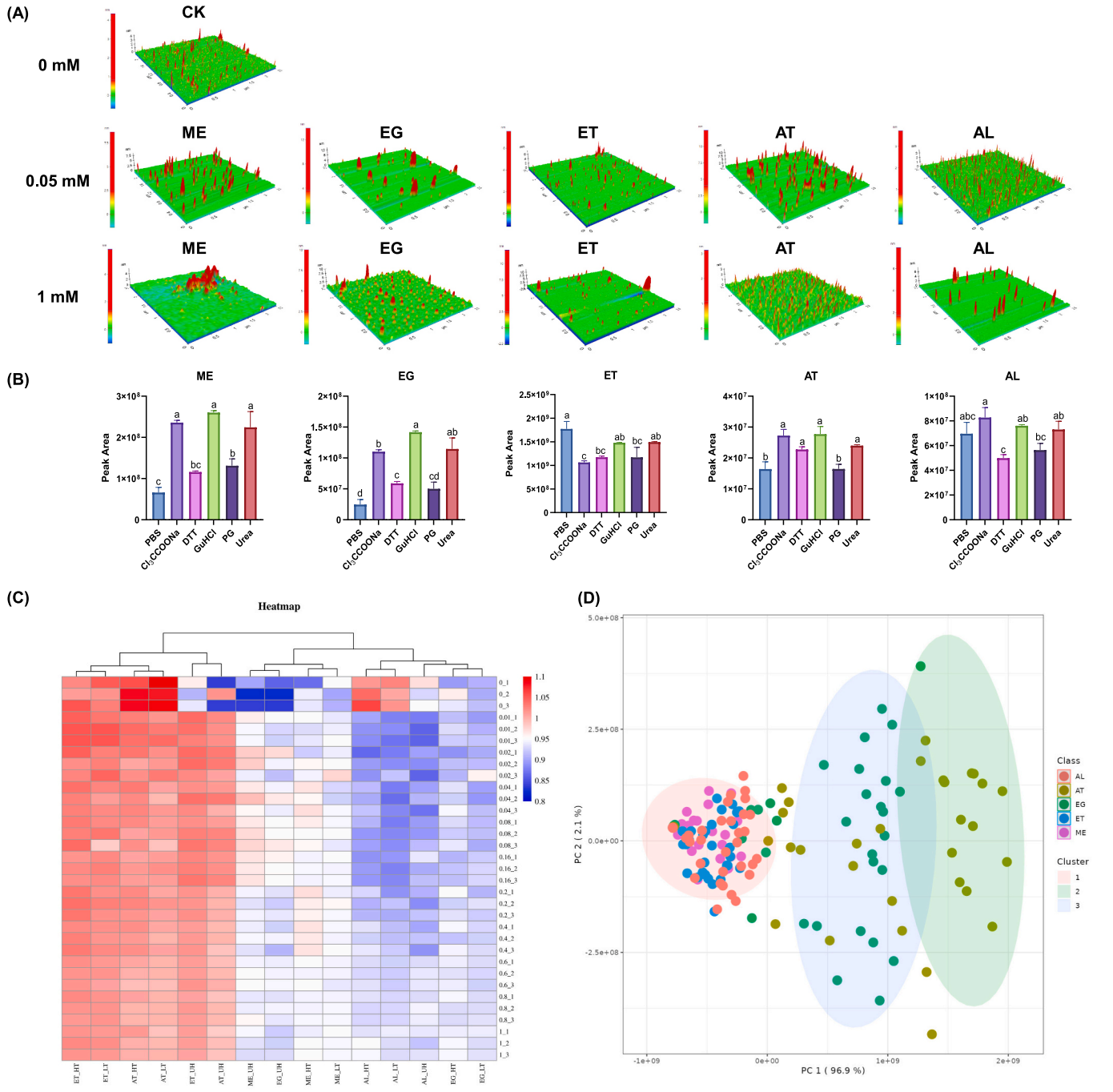

Fig. 3. (A) three-dimensional morphology of MPs, (B) peak areas under different chemical regents, (C) heatmap of flavor retention/release behavior, (D) K-means analysis results. CK, control group; ME, methyleugenol; EG, eugenol; ET, estragole; AT, anethole; AL, anisaldehyde. Columns with different letters indicate a significant difference ($P < 0.05$).

3.7. Analysis of the interaction behavior between MPs and PFCs

The interaction of PFCs with MPs is mainly influenced by their molecular structures and functional groups. According to Fig. 3-(B), ME, EG, ET, and AT primarily interact with MPs through non-covalent bonds, including hydrophobic interactions and hydrogen bonding. Non-covalent bonds can be disrupted or strengthened by $Cl_3CCOONa$, GuHCl, PG, and urea (Wang & Arntfield, 2016). The peak areas related to the concentrations of ME, EG, and AT after the addition of $Cl_3CCOONa$, GuHCl, and urea increased significantly, indicating that hydrogen bonds and hydrophobic interactions are critical for PFCs-MP binding (Bi et al., 2022). The retention of EG, which contains additional hydroxyl groups, increased significantly following PG addition, which may reduce the hydrophobic interactions and enhance the hydrogen bonding and ionic effects (Wang & Arntfield, 2016). Notably, the significant decrease in GC–MS peak areas (indicating enhanced binding) of ET with the addition of $Cl_3CCOONa$, DTT, and PG. The combined effects of protein unfolding (via $Cl_3CCOONa$ and DTT) and structural stabilization (via PG) might create an environment that enhances the retention of ET. Interestingly, AL exhibited a remarkably stable binding profile across all dissociating conditions. These treatments may not significantly alter surface-exposed polar binding sites where AL preferentially associates. Furthermore, the interaction between AL and MPs is likely dominated by hydrogen bonding rather than

hydrophobic interactions. These results are consistent with molecular docking (Fig. 4).

The binding behavior between PFCs and MPs at different concentrations was displayed in Fig. 3-(C). Interestingly, a salting-out effect was observed at lower concentrations. These observations are consistent with a previous study showing that the concentration-dependent salting-out effect caused by electrostatic repulsion in the MPs is stronger than that in PBS (Guo et al., 2020). Besides, adding PFCs may change the distribution of MP surface charges and hydration layers, which may also contribute to the observed salting-out effect. The cluster analysis based on the binding rates of the five PFCs under varying thermal treatments and concentrations revealed two distinct interaction patterns (Fig. 3-(D)). K-Means clustering is an unsupervised machine-learning algorithm that groups data to identify inherent ligand–protein interactions and enables unbiased clustering based on integrated interaction features (Osinomumu et al., 2025). The first cluster was AT and EG, whereas AL, ET, and ME grouped the second cluster. The observed tendency for two clusters may be attributed to their differences in binding ability (Table S3). EG possesses a phenolic hydroxyl group, which functions as both a hydrogen-bond donor and acceptor, thereby enabling stronger specific interactions with polar residues. EG and AT primarily interacted through hydrogen bonding (ASN187) and hydrophobic pockets (VAL186; PRO127) (Table S3). The methoxy substitution in ME may reduce the potential for hydrogen-bonding interactions. The allyl ether group of ET might exhibit a limited capacity to form strong hydrogen bonds. These structural features result in weaker ligand–protein interactions, producing smaller perturbations to MP conformation—consistent with earlier reports for low-affinity aroma molecules such as ketones and furans (Yin et al., 2022; Zhou et al., 2014). Typically, ketones interact with MPs through hydrophobic interaction (Wang et al., 2022). Furans, including furfuryl derivatives, also tend to exhibit low-affinity binding dominated by Hydrogen bond, van der Waals force, and hydrophobic interaction (Yin et al., 2022). In contrast, the PFCs examined in this study possess aromatic rings and phenoxy/methoxy substituents that facilitate stronger hydrogen bonding interactions with hydrophobic pockets of MPs. This finding is consistent with the more pronounced conformational effects observed here. This comparison underscores the mechanistic novelty of PFC–protein interactions relative to other classes of aroma compounds. The similarity in their thermal binding behavior suggested a similar binding mechanism, which still requires clarification through molecular simulation.

3.8. Molecular docking

Molecular docking was performed to elucidate the binding mechanism between MPs and PFCs. Previous studies have confirmed that proteins' internal cavities provide a highly hydrophobic environment along with accessible hydrogen bonding sites, which contribute to the stabilization of ligand-protein complexes (Gong et al., 2020; Yu et al., 2024). As shown in Table S3, the binding energies varied between −6.2 and − 6.8 kcal/mol, indicating that all five PFCs may bind within the internal cavity of MPs. As displayed in Fig. 4, PFCs can form hydrogen bonds and hydrophobic interactions with adjacent amino acid residues within the protein's docking site. Hydrogen bonds were essential for stabilizing these complexes. ASN187 was identified as a critical binding residue, forming hydrogen bonds with EG, ET, AT, and AL. Additionally, TYR115 participated in hydrogen bonding with EG and AL. ASN126 was the only hydrogen-binding residue of ME. Interestingly, despite AL forming the highest number of hydrogen bonds (three in total), it showed the lowest binding energy, suggesting that other non-covalent interactions, including hydrophobic and van der Waals interactions, also contribute significantly to determining the overall binding affinity. Among the configurations of five PFCs, the hydroxyl groups (–OH) function as both hydrogen bond donors and acceptors, which enhances their capacity to establish stable hydrogen-bond networks (Chen et al., 2020). The phenolic hydroxyl group of EG plays a vital role in its interaction with MPs. The hydrogen bonding potential of methoxy groups (-OCH_3) was considerably lower due to a greater steric hindrance. Additionally, it has been reported that methoxy groups (-OCH_3) are more likely to participate in hydrophobic or van der Waals interactions rather than hydrogen bonding (Lv et al., 2025). Hydrophobic interactions were primarily observed at the core hydrophobic pocket consisting of VAL186 and PRO127, which played a central role in PFCs binding. For ME, amino acid residues participating in hydrophobic interactions increased, which may result from the increase in methoxy groups. As regioisomers, AT and ET consist of the same molecular formula ($C_{10}H_{12}O$) and functional groups. However, subtle differences in the relative positions of the methoxy and propenyl groups on the aromatic ring influenced their binding behavior and energy. For AT, the methoxy and propenyl groups were arranged in the 1,4-substitution pattern, resulting in a more extended, linear molecular conformation. The trans-configuration carbon-carbon double bond improved spatial flexibility. Conversely, with a 1,2-substitution pattern of methoxy and propenyl groups and a cis-configuration carbon-carbon double bond, ET showed a compact, spatially constrained structure. In turn, steric hindrance limited its ability to conform to the hydrophobic pocket.

3.9. Mechanism inferences

Based on the experimental results, the proposed mechanism illustrating how structural features influence flavor binding capacity is presented in Fig. 5. The secondary structure results showed the transition from β-sheet to α-helix, resulting from enhanced intramolecular hydrogen bonding and destabilization of intermolecular interactions (Chen, Ma, et al., 2023; Chen, Zhao, et al., 2023). Thermal treatment leads to protein unfolding, exposing specific amino acid residues and reactive sites that are typically buried within the native tertiary structure. However, the addition of PFCs facilitated the re-embedding behavior of hydrophobic regions on the MPs' surface. This investigation revealed PFC-MPs binding behavior that is both structurally dependent and mechanistically distinct from ketones and furan derivatives. While ketones generally induce perturbations in MP conformation through hydrophobic interactions (Wang et al., 2022), and furan derivatives tend to cause ordered secondary structures to transform to random coil (Yin et al., 2022), the PFCs exerted stronger stabilizing effects on α-helical structures in the unheated state. The increase in α-helix content following the addition of PFCs suggests that the aromatic backbone and conjugated substituents of PFCs promote extensive hydrophobic packing and hydrogen bonding, enabling a more ordered intramolecular environment than that typically induced by ketones or furans. However, the effects of these substances were mitigated by prolonged thermal treatment. The application of heat resulted in an intensification of protein aggregation and a concomitant reduction in the availability of hydrophobic cavities. This phenomenon led to a diminution of the structural influence of PFCs in the heated state relative to the unheated state. The present results underscore that PFC–MP interactions are more sensitive to heat-induced occlusion of binding sites, owing to the bulkier phenylpropanoid skeleton. Consistent with the result of molecular docking and K-means clustering, hydrogen bonds and hydrophobic interactions were crucial for the PFCs' interaction with MPs. The configuration and conformation of PFCs influence their binding behavior with MPs. For example, the relative positioning of methoxy and propenyl substituents on the aromatic ring subtly modulated the binding behavior of AT and ET. The phenolic hydroxyl group plays a central role in EG-MP binding and structural alteration. Besides, as shown in Table S1, PFCs with higher Log *P* values exhibited a stronger propensity to interact with the exposed hydrophobic regions on the surface of MPs. PFCs with higher Log P values, indicating stronger hydrophobic character, likely promote protein–protein bridging through hydrophobic interactions, which accelerates the formation of larger aggregates. The formation of aggregation would influence the binding

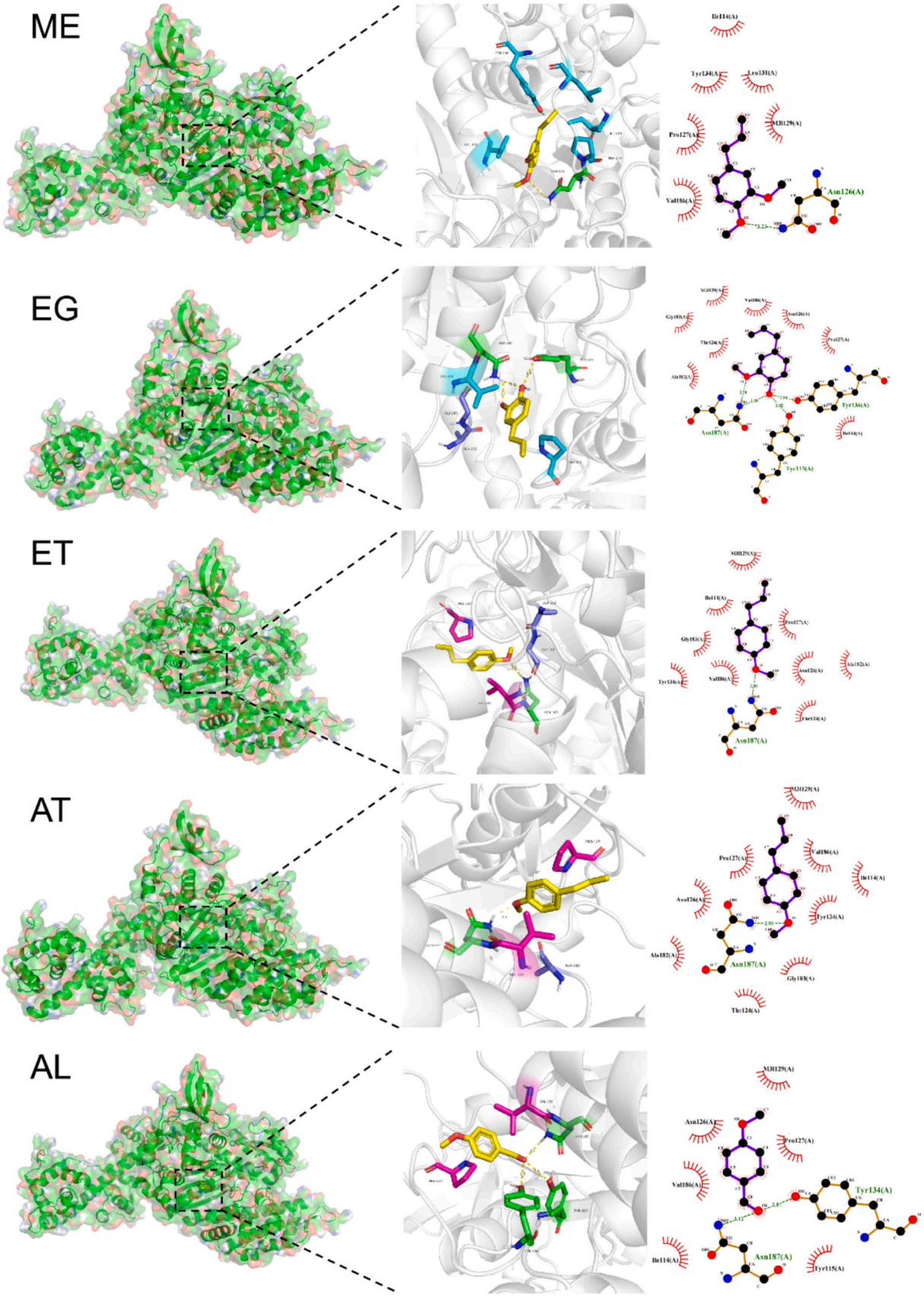

Fig. 4. Molecular interaction model of PFCs-Myosin.

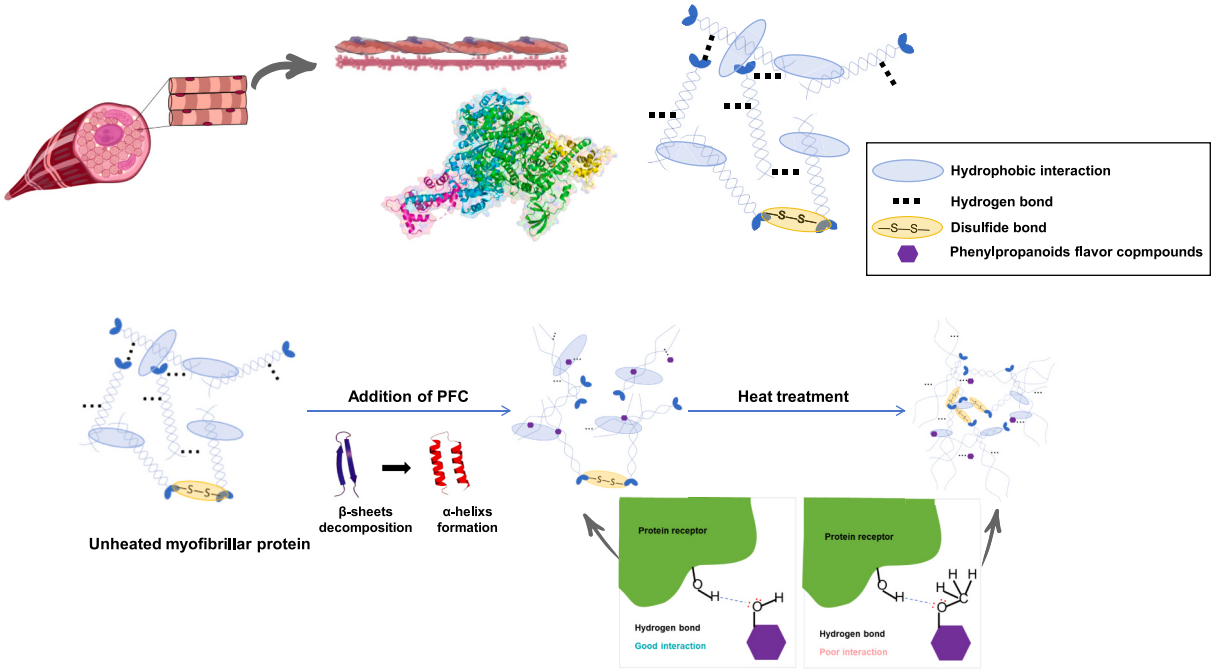

Fig. 5. Schematic modeling of the PFC-MP binding mechanism under different heat treatments.

behavior of PFCs. Furthermore, the disruption agent analysis provided complementary evidence of the interactions. Both DTT and $Cl_3CCOONa$ exhibited a significant positive correlation with BPB. The addition of DTT would disrupt the covalent cross-links, while $Cl_3CCOONa$ could destabilize protein structure by interfering with the hydrophobic domains (Wang & Arntfield, 2016. Both agents induced protein unfolding, leading to the exposure of hydrophobic regions that were previously buried within the protein core, resulting in higher surface hydrophobicity readings. Reduced BPB was found to diminish both the content of hydrophobic groups and the availability of binding sites for volatile compounds, which would promote flavor release extent (KuHn et al., 2008).

4. Conclusions

In conclusion, the present study elucidated the interaction mechanism between PFCs and MPs. The addition of PFCs increased the α-helix content of unheated MPs. However, prolonged heat treatment reduced the structural impact of PFCs, as increased protein aggregation limited the availability of binding sites. The chemical structure plays a crucial role in the binding behavior between PFCs and MPs. Consequently, EG mitigated heat-induced aggregation via non-covalent stabilization of reactive groups, while AL enhanced myosin heavy chain association and polymerization. As the concentration increased, the diminishing influence of EG became more pronounced. Furthermore, the unsupervised K-means machine-learning approach evaluated the binding behavior among the five PFCs to MPs. Two clusters were in accordance with the binding energy of molecular docking. Molecular docking analysis confirmed that hydrophobic interactions dominated the binding process, with hydrogen bonding playing supplementary roles. Additionally, structural differences among PFCs, particularly the presence of hydroxyl versus methoxy groups, influence their binding affinity for MPs by altering hydrogen bonding capacity and steric accessibility. The results provide comprehensive evidence that the flavor binding capacity of MPs is regulated by the interplay between protein conformational flexibility, surface hydrophobicity, ligand hydrophobicity, and the integrity of internal stabilizing forces. Subsequent studies should aim to validate these mechanisms in authentic meat systems under industrially relevant processing conditions. The investigation of competitive binding in multi-flavor environments and the integration of sensory analysis or in vivo oral processing approaches can also help to link molecular interactions with perceived flavor quality. These efforts will enhance the practical applications of molecular insights in flavor design during meat processing.

CRediT authorship contribution statement

Jingfan Wang: Writing – original draft, Software, Methodology, Data curation, Conceptualization. **Laiyu Zhao:** Writing – original draft, Data curation. **Ping Yang:** Writing – review & editing, Resources, Funding acquisition. **Tianze Wang:** Validation, Software. **Ying Xu:** Visualization, Investigation. **Dong Han:** Writing – review & editing, Visualization, Resources, Investigation, Funding acquisition. **Marie-Laure Fauconnier:** Writing – review & editing, Supervision. **Giorgia Purcaro:** Writing – review & editing, Supervision. **Chunhui Zhang:** Writing – review & editing, Supervision, Resources, Funding acquisition.

Declaration of competing interest

The authors declare that they have no known competing financial interests or personal relationships that could have appeared to influence the work reported in this paper.

Acknowledgments

This study was supported by the Agricultural Science and Technology Innovation Program (ASTIP-Y2025QC29), the National Natural Science Foundation of China (No. 32472392), the Agricultural Science and Technology Innovation Program of the Institute of Food Science and Technology, Chinese Academy of Agricultural Sciences (CAAS-ASTIP-Q2024-IFST-07), and the China Scholarship Council.

Appendix A. Supplementary data

Supplementary data to this article can be found online at https://doi.org/10.1016/j.foodres.2025.118268.

Data availability

Data will be made available on request.

References

Bi, S., Pan, X., Zhang, W., Ma, Z., Lao, F., Shen, Q., & Wu, J. (2022). Non-covalent interactions of selected flavors with pea protein: Role of molecular structure of flavor compounds. *Food Chemistry, 389*, Article 133044. https://doi.org/10.1016/j.foodchem.2022.133044

Bortnowska, G. (2022). Effects of composition and storage time of biopolymers-based emulsion-filled gels on the retention and release of aroma compounds: Thermodynamic and kinetic studies. *Food Chemistry, 382*, Article 132308. https://doi.org/10.1016/j.foodchem.2022.132308

Bortnowska, G. (2024). Aroma compounds retention and release from protein-polysaccharide-based bilayer emulsion gels: A thermodynamic and kinetic study. *Food Hydrocolloids, 150*, Article 109648. https://doi.org/10.1016/j.foodhyd.2023.109648

Cao, H., Jiao, X., Fan, D., Huang, J., Zhao, J., Yan, B., & Wang, M. (2019). Microwave irradiation promotes aggregation behavior of myosin through conformation changes. *Food Hydrocolloids, 96*, 11–19. https://doi.org/10.1016/j.foodhyd.2019.05.002

Chai, J., Xu, X., & Zhao, X. (2025). Effects of polysaccharides on the solubilization of myofibrillar protein in aqueous solution: A comparative study. *Food Hydrocolloids, 164*, Article 111193. https://doi.org/10.1016/j.foodhyd.2025.111193

Chen, H., Ma, J., Pan, D., Diao, J., Guo, A., Li, R., & Xiong, Y. L. (2023). Concentration-dependent effect of eugenol on porcine myofibrillar protein gel formation. *Meat Science, 201*, Article 109187. https://doi.org/10.1016/j.meatsci.2023.109187

Chen, H., Zhao, G., Yu, X., Zhang, Q., Zhu, C., Tong, L., & Hao, J. (2023). Exploring in vitro gastrointestinal digestion of myofibrillar proteins at different heating temperatures. *Food Chemistry, 414*, Article 135694. https://doi.org/10.1016/j.foodchem.2023.135694

Chen, J., Yang, J., Ma, L., Li, J., Shahzad, N., & Kim, C. K. (2020). Structure-antioxidant activity relationship of methoxy, phenolic hydroxyl, and carboxylic acid groups of phenolic acids. *Scientific Reports, 10*(1), 2611. https://doi.org/10.1038/s41598-020-59451-z

Cortés-Rojas, D. F., De Souza, C. R. F., & Oliveira, W. P. (2014). Clove (*Syzygium Aromaticum*): A precious spice. *Asian Pacific Journal of Tropical Biomedicine, 4*(2), 90–96. https://doi.org/10.1016/S2221-1691(14)60215-X

Dief, L. E., Eltamany, E. E., Abu-Elsaoud, A. M., Diri, R. M., Murshid, S. S. A., Al-Ghamdi, F., … Ibrahim, A. K. (2025). Development and validation of a RP-HPLC-DAD method for the simultaneous determination of estragole and trans-anethole in extracts, edible herbal products and commercial essential oils. *Microchemical Journal, 216*, Article 114572. https://doi.org/10.1016/j.microc.2025.114572

Dockal, M., Carter, D. C., & Ruker, F. (2000). Conformational transitions of the three recombinant domains of human serum albumin depending on pH. *Journal of Biological Chemistry, 275*(5), 3042–3050. https://doi.org/10.1074/jbc.275.5.3042

Ezugwu, A. E., Ikotun, A. M., Oyelade, O. O., Abualigah, L., Agushaka, J. O., Eke, C. I., & Akinyelu, A. A. (2022). A comprehensive survey of clustering algorithms: State-of-the-art machine learning applications, taxonomy, challenges, and future research prospects. *Engineering Applications of Artificial Intelligence, 110*, Article 104743. https://doi.org/10.1016/j.engappai.2022.104743

Ge, L., Xu, Y., Xia, W., & Jiang, Q. (2018). Synergistic action of cathepsin B, L, D and calpain in disassembly and degradation of myofibrillar protein of grass carp. *Food Research International, 109*, 481–488. https://doi.org/10.1016/j.foodres.2018.04.067

Gianelli, M. P., Flores, M., & Toldrá, F. (2003). Interactions of soluble peptides and proteins from skeletal muscle on the release of volatile compounds. *Journal of Agricultural and Food Chemistry, 51*(23), 6828–6834. https://doi.org/10.1021/jf0303666

Gong, S., Yang, C., Zhang, J., Yu, Y., & Wang, Z. (2020). Study on the interaction mechanism of purple potato anthocyanins with casein and whey protein. *Food Hydrocolloids, 111*(2), Article 106223. https://doi.org/10.1016/j.foodhyd.2020.106223

Guo, J., He, Z., Wu, S., Zeng, M., & Chen, J. (2020). Effects of concentration of flavor compounds on interaction between soy protein isolate and flavor compounds. *Food Hydrocolloids, 100*, Article 105388. https://doi.org/10.1016/j.foodhyd.2019.105388

Han, J., Du, Y., Yan, J., Jiang, X., Wu, H., & Zhu, B. (2021). Effect of non-covalent binding of phenolic derivatives with scallop (Patinopecten yessoensis) gonad protein isolates on protein structure and in vitro digestion characteristics. *Food Chemistry, 357*, Article 129690. https://doi.org/10.1016/j.foodchem.2021.129690

Han, P., An, N., Yang, L., Ren, X., Lu, S., Ji, H., & Dong, J. (2022). Molecular dynamics simulation of the interactions between sesamol and myosin combined with spectroscopy and molecular docking studies. *Food Hydrocolloids, 131*, Article 107801. https://doi.org/10.1016/j.foodhyd.2022.107801

Huang, X., Sun, L., Liu, L., Wang, G., Luo, P., Tang, D., & Huang, Q. (2022). Study on the mechanism of mulberry polyphenols inhibiting oxidation of beef myofibrillar protein. *Food Chemistry, 372*, Article 131241. https://doi.org/10.1016/j.foodchem.2021.131241

Jia, N., Wang, L., Shao, J., Liu, D., & Kong, B. (2017). Changes in the structural and gel properties of pork myofibrillar protein induced by catechin modification. *Meat Science, 127*, 45–50. https://doi.org/10.1016/j.meatsci.2017.01.004

Jia, N., Zhang, F., Liu, Q., Wang, L., Lin, S., & Liu, D. (2019). The beneficial effects of rutin on myofibrillar protein gel properties and related changes in protein conformation. *Food Chemistry, 301*, Article 125206. https://doi.org/10.1016/j.foodchem.2019.125206

Ju, Q., Yuan, Y., Wu, C., Hu, Y., Zhou, S., & Luan, G. (2023). Heat-induced aggregation of subunits/polypeptides of soybean protein: Structural and physicochemical properties. *Food Chemistry, 405*, Article 134774. https://doi.org/10.1016/j.foodchem.2022.134774

KuHn, J., Considine, T. R. S., & Singh, H. (2008). Binding of flavor compounds and whey protein isolate as affected by heat and high pressure treatments. *Journal of Agricultural and Food Chemistry, 56*(21), 10218–10224. https://doi.org/10.1021/jf801810b

Levine, R. L., Garland, D., Oliver, C. N., Amici, A., & Stadtman, E. R. (1990). Determination of carbonyl content in oxidatively modified proteins. *Methods in Enzymology, 186*, 464–478. https://doi.org/10.1016/0076-6879(90)86141-H

Li, L., Zhao, X., & Xu, X. (2022). Trace the difference driven by unfolding-refolding pathway of myofibrillar protein: Emphasizing the changes on structural and emulsion properties. *Food Chemistry, 367*, Article 130688. https://doi.org/10.1016/j.foodchem.2021.130688

Lou, X. W., Yang, Q. L., Sun, Y. Y., & Cao.. (2017). The effect of microwave on the interaction of flavour compounds with G-actin from grass carp (*Catenopharyngodon idella*). *Journal of the Science of Food and Agriculture, 97*(12), 3917–3922. https://doi.org/10.1002/jsfa.8325

Lv, G., Li, D., Bao, Y., Qin, Y., Zhang, X., Xu, F., & Zhang, Y. (2025). Effects of methoxy groups and carbon-carbon double bonds in phenolic acids on the physicochemical characteristics and digestibility of cassava starch. *Carbohydrate Polymers, 362*, Article 123687. https://doi.org/10.1016/j.carbpol.2025.123687

Miles, A. J., Ramalli, S. G., & Wallace, B. A. (2022). DichroWeb, a website for calculating protein secondary structure from circular dichroism spectroscopic data. *Tools for Protein Science, 31*(1), 37–46. https://doi.org/10.1002/pro.4153

Osinomumu, I. O., Reddy, U., Doretto, G., & Adjeroh, D. A. (2025). A survey of machine learning techniques in flavor prediction and analysis. *Trends in Food Science & Technology, 166*, Article 105339. https://doi.org/10.1016/j.tifs.2025.105339

Ozdal, T., Capanoglu, E., & Altay, F. (2013). A review on protein–phenolic interactions and associated changes. *Food Research International, 51*(2), 954–970. https://doi.org/10.1016/j.foodres.2013.02.009

Prodpran, T., Benjakul, S., & Phatcharat, S. (2012). Effect of phenolic compounds on protein cross-linking and properties of film from fish myofibrillar protein. *International Journal of Biological Macromolecules, 51*(5), 774–782. https://doi.org/10.1016/j.ijbiomac.2012.07.010

Promeyrat, A., Gatellier, P., Lebret, B., Kajak-Siemaszko, K., Aubry, L., & Santé-Lhoutellier, V. (2010). Evaluation of protein aggregation in cooked meat. *Food Chemistry, 121*(2), 412–417. https://doi.org/10.1016/j.foodchem.2009.12.057

Qian, R., Sun, C., Bai, T., Yan, J., Cheng, J., & Zhang, J. (2024). Recent advances and challenges in the interaction between myofibrillar proteins and flavor substances. *Frontiers in Nutrition, 11*, Article 1378884. https://doi.org/10.3389/fnut.2024.1378884

Schieber, A., & Wust, M. (2020). Volatile phenols-important contributors to the aroma of plant-derived foods. *Molecules, 25*(19). https://doi.org/10.3390/molecules25194529

Strauss, G., & Gibson, S. M. (2004). Plant phenolics as cross-linkers of gelatin gels and gelatin-based coacervates for use as food ingredients. *Food Hydrocolloids, 18*(1), 81–89. https://doi.org/10.1016/s0268-005x(03)00045-6

Sun, X., Saleh, A. S. M., Wang, Z., Yu, Y., Li, W., & Zhang, D. (2024). Insights into the interactions between etheric compounds and myofibrillar proteins using multi-spectroscopy, molecular docking, and molecular dynamics simulation. *Food Research International, 175*, Article 113787. https://doi.org/10.1016/j.foodres.2023.113787

Sun, X., Yu, Y., Saleh, A. S. M., Yang, X., Ma, J., Li, W., & Wang, Z. (2023). Understanding interactions among flavor compounds from spices and myofibrillar proteins by multi-spectroscopy and molecular docking simulation. *International Journal of Biological Macromolecules, 229*, 188–198. https://doi.org/10.1016/j.ijbiomac.2022.12.312

Tajima, M., Ito, T., Arakawa, N., & Parrish, F. C. (2006). Heat-induced changes of myosin and sarcoplasmic proteins in beef during simmering. *Journal of Food Science, 66*(2), 233–237. https://doi.org/10.1111/j.1365-2621.2001.tb11323.x

Wang, H., Zhang, H., Liu, Q., Xia, X., Chen, Q., & Kong, B. (2022). Exploration of interaction between porcine myofibrillar proteins and selected ketones by GC-MS, multiple spectroscopy, and molecular docking approaches. *Food Research International, 160*, Article 111624. https://doi.org/10.1016/j.foodres.2022.111624

Wang, J., Yang, P., Liu, J., Yang, W., Qiang, Y., Jia, W., & Fauconnier, M. L. (2024). Study of the flavor dissipation mechanism of soy-sauce-marinated beef using flavor matrices. *Food Chemistry, 437*, Article 137890. https://doi.org/10.1016/j.foodchem.2023.137890

Wang, K., & Arntfield, S. D. (2015). Binding of selected volatile flavour mixture to salt-extracted canola and pea proteins and effect of heat treatment on flavour binding. *Food Hydrocolloids, 43*, 410–417. https://doi.org/10.1016/j.foodhyd.2014.06.011

Wang, K., & Arntfield, S. D. (2016). Probing the molecular forces involved in binding of selected volatile flavour compounds to salt-extracted pea proteins. *Food Chemistry, 211*, 235–242. https://doi.org/10.1016/j.foodchem.2016.05.062

Wang, T., Han, D., Zhao, L., Huang, F., Yang, P., & Zhang, C. (2023). Binding of selected aroma compounds to myofibrillar protein, sarcoplasmic protein, and collagen during thermal treatment: Role of conformational changes and degradation of proteins. *Journal of Agricultural and Food Chemistry, 71*(46), 17860–17873. https://doi.org/10.1021/acs.jafc.3c02618

Wang, T., Wang, J., Han, D., Qiang, Y., Zhao, L., Xu, Y., & Zhang, C. (2024). Elucidating the adsorption mechanisms of yeast extract on trimethylamine and dimethylamine based on multi-spectroscopic techniques and molecular docking. *Journal of Molecular Liquids, 405*, Article 125087. https://doi.org/10.1016/j.molliq.2024.125087

Xiang, Q., Yao, L., Zhou, J., Li, S., Zeng, W., & Liu, P. (2025). Effects of heat treatment on the binding between the key aroma-active compounds in Zanthoxylum bungeanum oil and pork myofibrillar proteins (MPs). *Food Chemistry, 482*, Article 144209. https://doi.org/10.1016/j.foodchem.2025.144209

Xu, L., Zheng, Y., Zhou, C., Pan, D., Geng, F., Cao, J., & Xia, Q. (2022). A structural explanation for enhanced binding behaviors between β-lactoglobulin and alkene-aldehydes upon heat- and ultrasonication-induced protein unfolding. *Food Hydrocolloids, 130*, Article 107682. https://doi.org/10.1016/j.foodhyd.2022.107682

Xu, Q. D., Yu, Z. L., & Zeng, W. C. (2021). Structural and functional modifications of myofibrillar protein by natural phenolic compounds and their application in pork meatball. *Food Research International, 148*, Article 110593. https://doi.org/10.1016/j.foodres.2021.110593

Xu, Y., Dong, M., Tang, C., Han, M., Xu, X., & Zhou, G. (2020). Glycation-induced structural modification of myofibrillar protein and its relation to emulsifying properties. *Lwt, 117*, Article 108664. https://doi.org/10.1016/j.lwt.2019.108664

Xu, Y., Wang, R., Zhao, H., Yin, Y., Li, X., Yi, S., & Li, J. (2020). Effect of heat treatment duration on the interaction between fish myosin and selected flavor compounds. *Journal of the Science of Food and Agriculture, 100*(12), 4457–4463. https://doi.org/10.1002/jsfa.10486

Yang, C., Wu, G., Liu, Y., Li, Y., Zhang, C., Liu, C., & Li, X. (2024). Low-voltage electrostatic field enhances the frozen force of −12 °C to suppress oxidative denaturation of the lamb protein during the subsequent frozen storage process after finishing initial freezing. *Food Chemistry, 438*, Article 138055. https://doi.org/10.1016/j.foodchem.2023.138055

Yin, X., Gao, M., Wang, H., Chen, Q., & Kong, B. (2022). Probing the interaction between selected furan derivatives and porcine myofibrillar proteins by spectroscopic and molecular docking approaches. *Food Chemistry, 397*, Article 133776. https://doi.org/10.1016/j.foodchem.2022.133776

Yu, M., Zhuang, L., Xie, Q., Li, T., Song, H., Wang, L., & Zheng, C. (2024). Influences of human milk proteins on the release of human milk odors: Non-covalent interactions between α-lactalbumin and key odor skeleton compounds. *Food Hydrocolloids, 155*, Article 110235. https://doi.org/10.1016/j.foodhyd.2024.110235

Yu, Y., Yuan, M., Zhou, L., Liu, Y., Chen, Y., Wu, D., & Wang, J. (2025). Spice aldehydes improve emulsification stability of β-carotene by Schiff base reaction binding sodium caseinate as emulsion surface stabilizer. *Food Chemistry, 475*, Article 143305. https://doi.org/10.1016/j.foodchem.2025.143305

Yun, J. M., Jian, H. W., Xiang, L., Xian, B. X., Zhen, Y. W., Chao, W., & Liang, S. (2019). Effect of alkyl distribution in pyrazine on pyrazine flavor release in bovine serum albumin solution. *RSC Advances, 9*(63), 36951–36959. https://doi.org/10.1039/C9RA06720E

Zhang, J., Kang, D., Zhang, W., & Lorenzo, J. M. (2021). Recent advantage of interactions of protein-flavor in foods: Perspective of theoretical models, protein properties and extrinsic factors. *Trends in Food Science & Technology, 111*, 405–425. https://doi.org/10.1016/j.tifs.2021.02.060

Zhao, X., Qi, J., Fan, C., Wang, B., Yang, C., & Liu, D. (2022). Ultrasound treatment enhanced the ability of the porcine myofibrillar protein to bind furan compounds: Investigation of underlying mechanisms. *Food Chemistry, 384*, Article 132472. https://doi.org/10.1016/j.foodchem.2022.132472

Zhou, F., Zhao, M., Su, G., & Sun, W. (2014). Binding of aroma compounds with myofibrillar proteins modified by a hydroxyl-radical-induced oxidative system. *Journal of Agricultural and Food Chemistry, 62*(39), 9544–9552. https://doi.org/10.1021/jf502540p